ACS APPLIED MATERIALS & INTERFACES

Research Article

www.acsami.org

Self-Folding Thermo-Magnetically Responsive Soft Microgrippers

Joyce C. Breger,[†,⊥] ChangKyu Yoon,[‡] Rui Xiao,[§] Hye Rin Kwag,[†] Martha O. Wang,[∥] John P. Fisher,[∥] Thao D. Nguyen,[‡,§] and David H. Gracias*[,†,‡]

[†]Department of Chemical and Biomolecular Engineering, The Johns Hopkins University, 3400 N Charles Street, Baltimore, Maryland 21218, United States

[‡]Department of Materials Science and Engineering, The Johns Hopkins University, 3400 N Charles Street, Baltimore, Maryland 21218, United States

[§]Department of Mechanical Engineering, The Johns Hopkins University, 3400 N Charles Street, Baltimore, Maryland 21218, United States

[∥]Fischell Department of Bioengineering, University of Maryland, College Park, College Park, Maryland 20742, United States

Supporting Information

ABSTRACT: Hydrogels such as poly(*N*-isopropylacrylamide-*co*-acrylic acid) (pNIPAM-AAc) can be photopatterned to create a wide range of actuatable and self-folding microstructures. Mechanical motion is derived from the large and reversible swelling response of this cross-linked hydrogel in varying thermal or pH environments. This action is facilitated by their network structure and capacity for large strain. However, due to the low modulus of such hydrogels, they have limited gripping ability of relevance to surgical excision or robotic tasks such as pick-and-place. Using experiments and modeling, we design, fabricate, and characterize photopatterned, self-folding functional microgrippers that combine a swellable, photo-cross-linked pNIPAM-AAc soft-hydrogel with a nonswellable and stiff segmented polymer (polypropylene fumarate, PPF). We also show that we can embed iron oxide (Fe_2O_3) nanoparticles into the porous hydrogel layer, allowing the microgrippers to be responsive and remotely guided using magnetic fields. Using finite element models, we investigate the influence of the thickness and the modulus of both the hydrogel and stiff polymer layers on the self-folding characteristics of the microgrippers. Finally, we illustrate operation and functionality of these polymeric microgrippers for soft robotic and surgical applications.

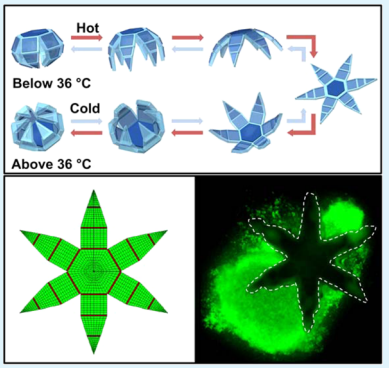

KEYWORDS: *smart materials, stimuli responsive materials, polypropylene fumarate, NIPAM, surgery, robotics*

INTRODUCTION

The ability to grip and securely hold onto objects is a vital task in robotics, manufacturing, and surgery. Conventional robots are composed of stiff materials such as metals (aluminum, steel) and ceramics (silicon, silicon oxide) with their joints being actuated using electrical, pneumatic, or hydraulic signals. Soft robotics is an emerging, bioinspired field that promises to augment the capabilities of traditional hard robotics with polymeric modules that mimic biological actuators.[1] As compared to their hard robotic counterparts, soft robotic structures have distinct advantages: they can be constructed using simple designs; be made lighter and inexpensively; be processed at low temperatures and in aqueous environments; and offer the possibility to mimic human functionality through their robotic functions.

Many previously described soft robotic actuators including those developed in the MEMS community are electrically or pneumatically driven.[1−7] For example, the reversible electrochemical swelling of polypyrrole in a variety of bilayer, trilayer, and sandwiched configurations has been used to create a number of folding and actuating structures.[4] More recently, a variety of pneumatically actuated robotic devices have been developed including a microhand for surgery,[5] networks capable of intricate motion,[1] and a universal gripper based on granular materials.[7] While these devices offer significant advantages in terms of the control, speed, universality, and momentum, their need for tethers as well as electrical power or gas sources can increase their weight and complexity. This limits their applicability in small or confined spaces or during repetitive actuation over long time periods.

The use of stimuli responsive mechanisms provides an alternative to tethered actuation and offers the possibility for smart behaviors such as autonomous responses in specific environments.[8−12] Many of these schemes employ hydrogels since these materials are able to swell significantly in response to a variety of stimuli such as temperature, light, or chemical reactions generating the energy and force to perform mechanical tasks.[13−15] Hydrogel actuators can also be created

Received: December 6, 2014
Accepted: January 16, 2015
Published: January 16, 2015

DOI: 10.1021/am508621s
ACS Appl. Mater. Interfaces 2015, 7, 3398−3405

using bigel strips composed of partially interpenetrated hydrogel networks with differing swelling properties. This concept was first demonstrated using bilayers of pNIPAM and acrylamide that had drastically different swelling behavior in response to temperature or aqueous environments.[16] The use of stimuli responsive bilayers has recently been combined with photo-cross-linking approaches to create a range of micro-structured actuators and self-folding devices.[10,11,17−21]

In our previous work on self-folding microactuators, we have demonstrated a range of self-assembled, origami-inspired structures that spontaneously fold-up and actuate from two-dimensional patterns without the need for any wires or external controls.[9,10,22−25] These structures utilized a variety of actuation forces derived by the minimization of surface tension; the release of residual stress triggered by light, enzymes, biochemicals, or temperature; and differential swelling based on pH or temperature changes. It is particularly noteworthy that previously created metallic microgrippers were autonomously actuated on introduction into the gastrointestinal tract of live pigs and used to biopsy tissue.[24] In order to enhance biocompatibility and possibly endow biodegradability in such surgical applications and for robotics, we believe there is a pressing need to develop polymeric, origami-inspired, and stimuli responsive microgripper structures.[9,22,25,26]

We have observed that one of the significant limitations of stimuli responsive hydrogel actuators is their low stiffness. For example, when we previously designed microgrippers composed of cross-linked pNIPAM-AAc alone, we observed that these grippers were very floppy and unable to securely grip onto beads which would often fall out of their grasp.[26] In order to address this limitation, we previously introduced the concept of combining rigid polymer segments of a nonswellable polymer to increase the overall stiffness of the pNIPAM-AAc polymer.[25] In this paper, we build on these earlier results to design, fabricate, and characterize mass-producible micro-grippers capable of cell excision. We have incorporated nanoparticle doping and a sequential photolithographic approach to create large numbers of autonomous, polymer-hydrogel bilayer grippers. These grippers have numerous advantageous properties including the capability for magnetic direction, simultaneous actuation based on temperature, independent function, optical transparency, and gripping onto and isolating tissue. Over numerous cycles, the resulting grippers can fold completely in either direction on the basis of temperature and fold reversibly. We use finite element analysis to model the folding behavior of these soft robotic grippers to gain insight into the influence of important material and design considerations such as polymer thickness and modulus.

The characteristics, thermal responsiveness, and stiffness were chosen for the polymer materials of the grippers based on their relevance for biological applications. pNIPAM is a thermoresponsive hydrogel that undergoes a low critical solution temperature (LCST) above physiological temperature where the polymer becomes hydrophobic expelling water and losing 90% of its mass while below its LCST, the polymer is hydrophilic and absorbs water.[27] The absorption and desorption of water in response to temperature serves as the actuation mechanism, and pNIPAM has been used extensively in drug delivery applications, cell culture, and tissue engineering applications.[28−33]

We have addressed the issue of pNIPAM biocompatibility in a previous publication.[25] Essentially, the backbone of pNIPAM hydrogels is not degradable although specific cross-linkers used to network the hydrogel can endow biodegredability.[28,31] Therefore, a networked pNIPAM hydrogel can be created with tunable degradation rates based on cross-linker density and type. PPF, a material originally designed for filling bone defects and similar in tensile strength to trabecular bone,[34,35] serves as a stiff and restrictive construct, mimicking phalanges in the human hand around which pNIPAM-AAc can contract or expand. The biodegradation products of PPF are propylene glycol and fumaric acid which are naturally expelled through the Krebs's cycle.[36]

Both PPF and pNIPAM are photopatternable and have been used previously in lithographic applications as well as to create therapeutic grippers or "theragrippers" in our own laboratory. By cross-linking, one can tune the physical and mechanical properties of the polymers without chemical modifications to the polymer backbone which can affect its biocompatibility.[37] The main advantage of photo-cross-linking over other cross-linking techniques is the ability to spatially and temporally control polymerization using photomasks and by varying the intensity of light. Further, a wide range of portable UV sources are available, and fast curing rates are achievable at room temperature. Photopatterned hydrogels can also be created over a wide range of sizes: we have previously created metallic microgrippers as small as a few hundred microns from tip to tip so that they can grip onto small sized cargo or pass through conventional catheters used in surgery.[24] All that is needed is the optimization of spacing between grippers, spacing of the rigid segments, and thickness of the hydrogel and stiff segment layers.

Magnetic fields are biocompatible even at clinically relevant but high field strengths; therefore, they offer many attractive advantages over other propulsion and guidance schemes.[38] Numerous examples of magnetically directed robotic devices have been developed for *in vivo* applications including metallic microgrippers, microdrillers, modified bacteria, and micro-swimmers.[21,22,38−40] Polymer microstructures can be made responsive to an electromagnetic field by incorporating magnetic nanoparticles within their network.[21,41,42] In this work, we have directly incorporated magnetic nanoparticles into the pNIPAM-AAc trigger layer, allowing for remote direction while keeping the arms free to grip onto and/or isolate tissue at a desired location.

MATERIALS AND METHODS

Materials. *N*-Isopropylacrylamide monomer (NIPAM, Scientific Polymer Products Inc.), poly-*N*-isopropylacrylamide (pNIPAM, MW 300 000, Scientific Polymer Products Inc.), *N*,*N*′-methylenebis-acrylamide (BIS, Sigma-Aldrich), n-butanol (Sigma-Aldrich), acrylic acid (AAc, Sigma-Aldrich), diethyl fumarate (DEF, Sigma-Aldrich), 80% hydrolyzed poly(vinyl alcohol) (PVA, MW 9−10 kDa, Sigma-Aldrich), iron(III) oxide (Sigma-Aldrich), Irgacure 2100 (Ciba), 1827 photoresist (Microchem), 351 developer (Microchem), and three inch silicon (Si) wafers (WRS) were used as is without further modification.

Synthesis of Polypropylene Fumarate (PPF). PPF was synthesized by a previously published method[34] and determined to have a MW of 804 Da and a polydispersity of 1.21.

Synthesis of pNIPAM-AAc. A NIPAM-AAc solution was prepared as described previously.[22] Briefly, 3 g of NIPAM monomer, 0.4 g pNIPAM, and 0.18 g BIS were dissolved overnight in 7.5 mL of n-butanol under constant stirring at room temperature. To this solution, 0.3 mL of AAc was added followed by 0.1 g of Irgacure 2100. The resultant mixture was stirred until the additives had been completely incorporated.

Profilometry. Glass slides were repeatedly washed with acetone, methanol (MeOH), and isopropyl alcohol (IPA) after which they were

DOI: 10.1021/am508621s
ACS Appl. Mater. Interfaces 2015, 7, 3398−3405

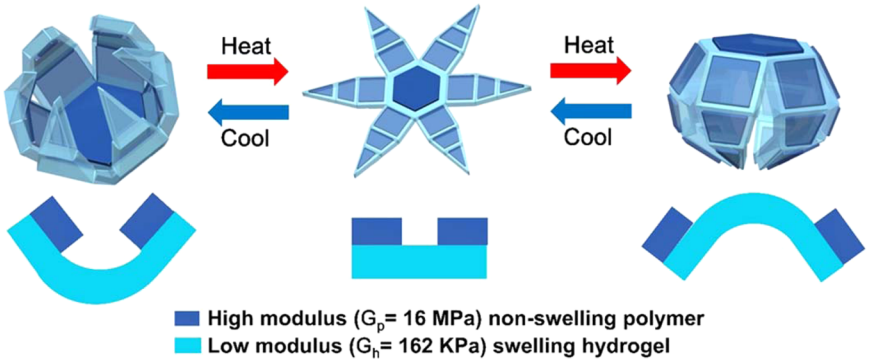

Figure 1. Schematic diagram illustrating the reversible self-folding of soft microgrippers in response to temperature. The photopatterned microgrippers are composed of stiff PPF segments atop a pNIPAM-AAc layer. Above 36 °C, the pNIPAM-AAc layer excludes water and contracts which causes the grippers to first open and then close such that the PPF segments face outward. Below 36 °C, the pNIPAM-AAc absorbs water and swells which causes the microgripper to open and then close in the opposite direction such that the pNIPAM-AAc layer faces outward.

dried with compressed air. A strip of cellophane tape was fixed to the middle of the glass slide making sure the edges where pressed down. A 3:1 w/w mixture of PPF/DEF with approximately 1% of Irgacure 2100 was added to the top of each glass slide. The PPF/DEF solutions were spin coated at varying speeds (500−3000 rpm) following which the tape was carefully removed. The polymer was UV cross-linked by varying amounts of UV (650−2600 mJ/cm^2) flood exposure through a glass mount with a mask aligner. The slide was then incubated and washed with ethanol (EtOH) followed by deionized (DI) H_2O to remove any unreacted components and dried under compressed air. Cross-linked polymer thickness was measured utilizing a profilometer. Measurements were taken in four different spatial locations of the glass slide and averaged for each thickness.

Photopatterning of pNIPAM-AAc Films. A sacrificial layer was deposited onto a Si wafer by spin coating a filtered (5 μm), 30% w/w PVA (1000 rpm for 1 min) aqueous solution and allowed to dry at 150 °C for 1 min. pNIPAM-AAc films (20 × 5 × 1 mm^3) for determining the volumetric swelling ratio were fabricated by first depositing 1 mL of NIPAM-AAc on top of a 3 in. Si wafer which was then rotated by hand to evenly spread out the NIPAM-AAc solution and allowed to rest for 1 min to obtain a uniform NIPAM-AAc thickness. The films were photopatterned utilizing a dark field mask and a mask aligner in noncontact mode (i.e., spacers approximately 3 mm thick were used between the mask and the sample) and exposed to 100 mJ/cm^2 UV light to initiate cross-linking. Unreacted components were removed by multiple washes with EtOH and MeOH and then finally washed once with DI H_2O. The cross-linked pNIPAM-AAc films were lifted off by placing the wafer in DI H_2O overnight.

Fabrication of Thermo-Magnetically Responsive Grippers. Alignment markers were photopatterned onto Si wafers utilizing negative photoresist, a dark field mask, and mask aligner. Cr (20 nm) and Cu (100 nm) were evaporated on the Si wafers, after which excess Cr, Cu, and photoresist were removed by sonication of the wafer in acetone. The wafers were rinsed with copious amounts of acetone, EtOH, MeOH, and IPA followed by drying with compressed air. A sacrificial, transparent PVA layer was deposited onto a Si wafer as described previously. These wafers were subsequently used for photopatterning polymeric structures.

To fabricate polymeric grippers, warm (~70 °C) PPF solution (3:1 PPF/DEF with approximately 1% w/w Irgacure 2100) was deposited onto the wafer, spread utilizing a spatula then spin coated at 3000 rpm to achieve a film approximately 10 μm thick. PPF segments were photopatterned utilizing a dark field mask and a mask aligner in noncontact mode and exposed to 650 mJ/cm^2 UV light to initiate cross-linking. A solution of NIPAM-AAc (1 mL) was deposited on top of the wafer, and the wafer was slowly rotated by hand to spread out the NIPAM-AAc evenly, and allowed to sit for 1 min to achieve uniform thickness before being exposed to 100 mJ/cm^2 UV light through a dark field mask that was the outline of the structure in noncontact mode as described previously. Unreacted PPF/DEF and NIPAM-AAc were removed by repeated EtOH and MeOH washes followed by a single final DI H_2O wash. The wafer was then immersed in DI H_2O to completely dissolve the PVA sacrificial layer. Grippers were collected into a 20 mL scintillation vial, rinsed with DI H_2O, and then stored in DI H_2O at 4 °C until use. Structures were made ferromagnetic by incorporating 5% w/w Fe_2O_3 into the NIPAM-AAc solution before spin coating and photopatterning.

Modeling of Swelling/Deswelling of the Soft-Microgrippers. In order to determine the swelling ratio, pNIPAM-AAc films were placed in fresh DI H_2O and incubated at 4 °C for 1 h to reach their equilibrium swollen state. Specimens were then removed from DI H_2O, blotted with a tissue, and weighed (n = 8). Specimens were placed back in DI H_2O and incubated at 27, 31, 33, 35, 37, and 40 °C. Afterward, the specimens were weighed again in the same manner as described previously. The swelling ratio (SR) or its inverse function, $1/\varphi$, was then calculated. We use the following definition for these quantities: $R = 1/\varphi = W_{swollen}/W_{dry}$.

The Young's moduli of swollen PPF and pNIPAM-AAc were measured using a dynamic mechanical analyzer Q800 (TA Instruments). The specimens were tested at room temperature in the dynamic mode with a frequency sweep from 0.1 to 10 Hz under a 0.2% applied strain for PPF and a 1% applied strain for pNIPAM-AAc. The storage modulus at 0.1 Hz was used to represent the Young's modulus for low strain rates since the storage modulus was an order of magnitude larger than the loss modulus at this low frequency.

Cell Culture. L929 (ATCC CCL-1; American Type Culture Collection, Manassas, VA), a fibroblast murine cell line, were stored at −80 °C. Aliquots were rapidly thawed and cultured in 5% CO_2/95% air, 70% humidity, at 37 °C in complete media (RPMI supplemented with 10% fetal bovine serum) until they adhered to the culture flask and reached 80−90% confluence (usually 2−3 days). The monolayer was harvested by washing the flask 3 times with 5 mL phosphate buffered saline (PBS) and then incubated in the presence of 0.25% (w/v) Trypsin until the cells became rounded and detached from the bottom of the flask (usually 3−5 min). The cells were centrifuged at 1000 rpm for 3 min to remove trypsin and resuspended in cold PBS. The cells were incubated on ice for 45 min in the presence of 2 mM calcein AM to stain the cells. Afterward the cells were centrifuged again at 1000 rpm for 5 min to remove excess dye and to create a L929 tissue-like pellet.

Polymeric Gripping of Tissue. Grippers were incubated at 4 °C or on ice to achieve a closed formation and were carefully dripped on top of each tissue pellet in warm PBS (~37 °C). The grippers immediately opened and were allowed to close around the tissue pellet (usually within 5 min). After closure, tissue filled grippers were retrieved with a transfer pipet and visualized. The gripper progress of closing around the tissue pellet was monitored with an AZ-100 fluorescent microscope. Time lapse images were taken every 2 s until the gripper closed completely.

DOI: 10.1021/am508621s
ACS Appl. Mater. Interfaces 2015, 7, 3398−3405

RESULTS AND DISCUSSION

Design and Fabrication of the Grippers. Our design is based on the combined use of stimuli responsive polymers such as pNIPAM-AAc with a degradable yet stiff polymer like PPF to increase rigidity of the actuator. Polymeric grippers were fabricated using sequential photolithography and fold into 3-D structures based on the swelling/deswelling through water absorption/desorption in response to temperature (Figure 1). The pNIPAM-AAc layer serves as a thermally responsive swelling hydrogel layer with a low shear modulus (G_h = 162 KPa) while the PPF layer serves as the nonswelling, restrictive layer with a much higher shear modulus (G_p = 16 MPa). Similar moduli values were previously reported for PPF mixed with ceramic materials showing compressive strengths ranging from 2 to 30 MPa.[43]

We used a serial photolithographic method to pattern the PPF/pNIPAM-AAc microgrippers (Figure 2, Supporting Information Figure 1). It is noteworthy that PPF is typically used in gram quantities for filling bone defects and photopatterning of this material is relatively new. Hence, it was necessary to develop methods to precisely control the thickness and lateral resolution of photopatterned PPF films. Specifically, we varied the spin coat speed, the UV intensity, and the spacing between PPF patterns to reliably mass produce well-structured microgrippers (details in Supporting Information Figure 1). We also note that since the PPF/DEF solution is much more viscous than the NIPAM-AAc solution, it is preferable to pattern the PPF/DEF solution first followed by NIPAM-AAc photopatterning. We observed that when patterned second, the PPF/DEF solution can dislodge the underlying patterned pNIPAM-AAc structures during spin coating. We also intentionally did not develop the PPF patterns before the addition of the NIPAM-AAc solution. It is noteworthy that delamination of bilayer actuators is a concern during reversible swelling and deswelling cycles. In our case, due to the material properties and processing, we observed sufficient adhesion between the two films, and we attribute it to two factors. First, the n-butanol in the NIPAM-AAc solution could partially develop the underlying PPF leading to polymer chain entanglement. Second, the reaction between the alkene functional groups of NIPAM, acrylic acid, DEF, and PPF could lead to improved adhesion at the interface.

Characterization of Gripper Folding. Once released from the wafer and equilibrated in solution, the polymeric structures were thermally responsive and could fold in both directions as shown in Figure 3A and in Supporting Information Movie 1 (am508621s_si_002). The literature LCST value for pNIPAM lies between 30 to 35 °C;[27] however, it is known that the LCST can be altered by copolymerization of NIPAM with other monomers as in pNIPAM-AAc.[31,44] We observed the self-folding transition temperature to be approximately 36 °C. We rationalize self-folding by noting that above this temperature pNIPAM-AAc is hydrophobic, the polymer collapses causing the gripper to close with the PPF segments on the outside of a closed gripper. Since the pNIPAM-AAc layer is opaque during polymer chain collapse, the transition can be readily observed under a microscope. As the temperature cools below 36 °C, the pNIPAM-AAc layer becomes clear and swells as it absorbs water causing it to open and then close in the opposite direction, now with the PPF segments on the inside of the gripper, as verified over 50 cycles.

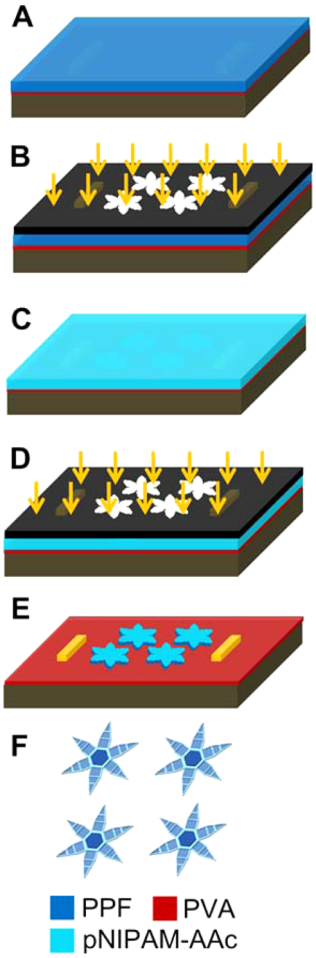

Figure 2. Schematic diagram of the PPF/pNIPAM-AAc microgripper fabrication process flow. (A) Metal alignment markers were evaporated onto a silicon wafer and a poly(vinyl alcohol) (PVA) sacrificial layer and PPF/DEF solution was deposited by spin coating. (B) Using a conventional mask aligner UV light was irradiated onto the PPF solution through a dark field mask to cross-link the PPF segments. (C) A layer of pNIPAM-AAc was added on top of the wafer and leveled by hand. (D) A second UV exposure through a dark field mask was used to photopattern the pNIPAM-AAc layer. (E) The uncross-linked PPF, DEF, NIPAM-AAc were removed by developing the wafer in alcohol (EtOH and/or MeOH) and DI H_2O. (F) The microgrippers were released from the wafer by placing the wafer in DI H_2O to dissolve the underlying PVA sacrificial layer.

We developed constitutive models for finite element simulation of the pNIPAM-AAc and PPF bilayer grippers (Supporting Information Figure 2) to study the influence of various design parameters on gripper folding and unfolding [Supporting Information Movies 2 and 3 (am508621s_si_003 and am508621s_si_004)]. The model was implemented into the open-source finite element code TAHOE (Sandia National Laboratories). As shown in Supporting Information Figure 2, the mesh was discretized using trilinear hexahedral elements, and a mesh convergence study was also performed to decide the mesh density. Self-folding results from the model are shown in Figure 3B as a function of temperature and the ratio of dry to swollen hydrogel weight (φ): the ratio φ increases with increasing temperatures as water is expelled. The simulation model is based on the thermodynamic framework for equilibrium mechanics coupled with hydrogel swelling[26] to describe the thermoresponsive behavior of the pNIPAM-AAc

DOI: 10.1021/am508621s
ACS Appl. Mater. Interfaces 2015, 7, 3398−3405

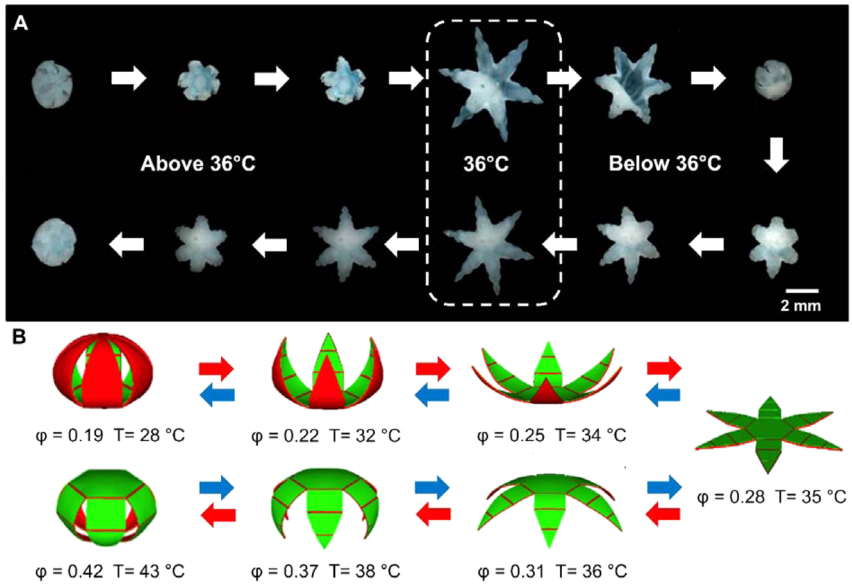

Figure 3. Experimental and simulation image snapshots from Supporting Information Movies 2 and 3 (am508621s_si_003 and am508621s_si_004) illustrating reversible thermally responsive self-folding of a representative microgripper in DI H_2O. (A) Images of a closed gripper with PPF segments on the outside opening as the temperature is decreased below 36 °C and then folding back on itself to become a closed gripper but with the PPF segments on the inside. On heating the self-folding process reverses, and reversibility was verified over 50 cycles (data not shown). In the absence of any thermal gradients associated with heating the grippers, we estimate the experimental time scale for actuation on the order of minutes. (B) Simulation snapshots are in agreement with the experimental trends and suggest that the extent of gripper folding depends on the temperature and the swelling function φ.

layer. The free energy of the hydrogel is assumed to be the sum of a mechanical part, represented by a Neo-Hookean model for the entropy elasticity of the polymer network with Gaussian chain statistics and a component for the energy of mixing represented by the Flory–Huggins model.[45] The Flory–Huggins parameter increases sigmoidally with temperature. The low-temperature and high-temperature values along with the transition temperature range were determined from the temperature-dependent swelling experiments described in the Materials and Methods section. The effect of diffusion through the micrometer-scale thick hydrogel layer was neglected, and we assumed the hydrogel was at equilibrium for each test temperature. A Neo-Hookean model was also applied to describe the mechanical behavior of the PPF layer. The shear modulus of the two layers was determined by dynamic mechanical analysis (DMA) described in the Materials and Methods section. Simulation snapshots in Figure 3B capture the opening and closing behavior of the grippers with the pNIPAM-AAc film on the inside of the grippers at high temperatures, and the trends agree with experimental data.

We also applied the model to investigate the effect of the gap between PPF segments, thickness, and modulus on the temperature-dependent folding configuration. Specifically, we varied the spacing between adjacent PPF segments on the gripper arms from 20 to 90 μm and found that this had a negligible effect. A smaller spacing between the rigid segments led to only slightly more folding. In contrast, both the thickness and modulus of the layers had a pronounced effect. In order to quantify the extent of folding as a function of these parameters, we plotted the ratio of the overall diameter of the grippers in the folded state (D) to the unfolded, flat diameter (D_o) while varying these parameters (Figure 4). A smaller value of (D/D_o) signifies greater folding. The thickness of PPF and pNIPAM-AAc was varied between half to twice the experimental thickness used, i.e., from 5 to 20 μm for PPF and 10 to 100

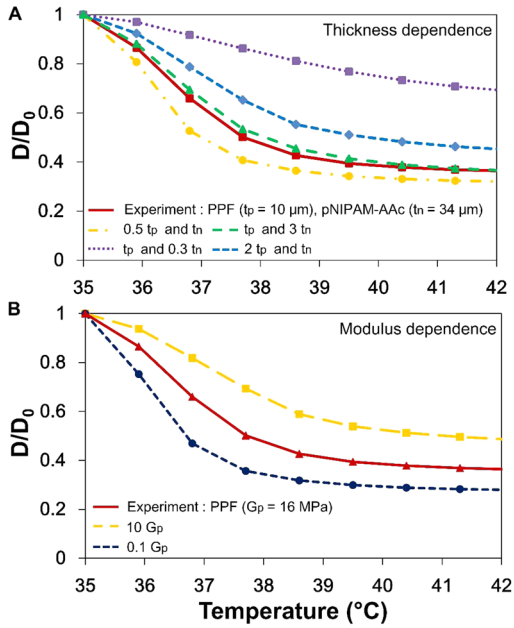

Figure 4. FEM sensitivity analysis exploring the dependence of the microgripper diameter reduction ratio (D/D_o) on the (A) thickness of the pNIPAM-AAc and PPF layers and (B) the modulus of the stiff layer.

μm for pNIPAM-AAc (Figure 4A). The thickness of PPF (t_p) used in experiments was approximately 10 μm while the thickness of pNIPAM-AAc (t_n) used was approximately 34 μm when swollen. Increasing the PPF layer thickness results in a higher (D/D_o) ratio signifying lower folding which we attribute to a higher bending rigidity of the PPF. However, the effect of varying the thickness of the pNIPAM-AAc layer is more complicated. For example, when the thickness of pNIPAM-AAc

DOI: 10.1021/am508621s
ACS Appl. Mater. Interfaces 2015, 7, 3398–3405

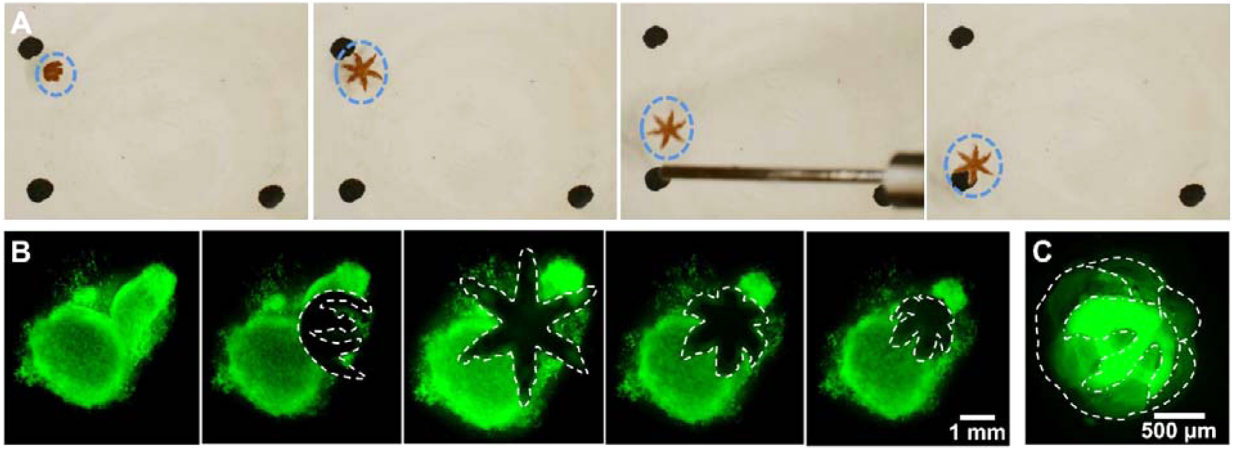

Figure 5. Applications of the soft thermoresponsive self-folding grippers. (A) Video snapshots showing guidance of Fe_2O_3 doped polymer grippers between two round black marks using a magnetic probe. (B) Capture and excision of cells from a live cell fibroblast clump. (C) Gripper with excised cells within its grasp. The dashed lines are added to aid visualization of the gripper and the excised cells.

is increased from 34 to 100 μm, the folding decreased only slightly, but when the thickness of pNIPAM-AAc is decreased from 34 to 10 μm, the folding also decreased but in a significantly more pronounced manner. We rationalize this result by noting that thin pNIPAM-AAc layers could not exert enough force to compress the stiffer PPF layers and bend the gripper arm while very thick pNIPAM-AAc layers were negligibly affected by the PPF layer. In order to find the optimum thickness of the pNIPAM-AAc layer, we ran an additional set of parameter studies by changing the thickness of pNIPAM-AAc layer while keeping the PPF layer thickness 10 μm. Our results suggest that the optimum thickness for the pNIPAM-AAc is then around 45 μm.

One of the important advances in this study is the validation of the hypothesis that bilayers composed of a high modulus layer with a hydrogel could increase the overall stiffness of the soft robotic tool. Hence, we simulated and compared self-folding ratios for a bilayer microgripper composed of a fixed pNIPAM-AAc modulus (=162 KPa) as a function of varying modulus of the stiff polymer layer ranging from the experimentally used PPF polymer modulus (G_p) of 16 MPa to hypothetical layers with 0.1 and 10 times this modulus, 1.6 and 160 MPa, respectively (Figure 4B). We observed that decreasing the modulus of the PPF by a factor of 10 led to tighter folding but also resulted in inhomogeneous folding and warping. Increasing the modulus of the stiff layer to 10 times that of the PPF resulted in decreased folding due to increased bending rigidity. Our simulations indicate that a modulus of about 16 MPa for PPF or any other stiff polymer would work best. Currently, we are working on a contact model to investigate the force between the gripper and tissue using the finite element method. We are also trying to develop experimental methods to characterize the contact force for verification of the numerical model.

Applications of the Grippers. The soft microgrippers can be made magnetic through the incorporation of iron oxide (Fe_2O_3) into one of the polymeric layers. Here, 5% w/w Fe_2O_3 was incorporated into the pNIPAM-AAc layer to achieve better dispersion of the Fe_2O_3 throughout the layer as compared to incorporation into the PPF layer. As shown in Supporting Information Movie 4 (am508621s_si_005), these polymeric grippers open in unison in response to temperature. The Fe_2O_3 particles provide contrast in visualizing the polymeric grippers which orient themselves in a magnetic field [Supporting Information Movie 5 (am508621s_si_006)]. The incorporation of Fe_2O_3 into the pNIPAM-AAc layer did not affect folding or photopatterning. By placing an external magnet near the desired location, the gripper can be guided toward that location (Figure 5A). Hence, they could potentially be directed or retrieved using a magnetic guide wire in a clinical setting as was done previously with ferromagnetic metallic grippers.[24]

Importantly, due to increased stiffness of the grippers, we observed that they were able to grip and excise cells from a fibroblast cell clump [Figure 5B and Supporting Information Movie 6 (am508621s_si_006)]. Fibroblasts are cells found in connective tissue. In these experiments, the grippers were stored at 4 °C so that they folded completely due to maximal absorption of water by the pNIPAM-AAc layer. The grippers were pipetted on top of a fibroblast clump and allowed to open up and then close in warm PBS (~37 °C) around the tissue, gripping it. The gripper is outlined with a dotted white line to aid in visualization of the gripper. The cells were stained with the Calcein AM, a commonly used stain to indicate live cells, and fluoresced bright green. A pipet was used to retrieve the grippers, and they were visualized with microscopy. After retrieval, we observed cells within the arms of the grippers. The fluorescent green live cells can be visualized through the transparent gripper arms (Figure 5C).

CONCLUSION

The goal of this study was to create and model stimuli responsive self-folding soft microgrippers composed of a continuous low modulus actuator layer of pNIPAM-AAc and stiff segments composed of PPF. pNIPAM-AAc was chosen as an appropriate actuator material based on its stimuli responsive properties and its method of actuation by swelling and deswelling in aqueous environments. We have validated the hypothesis that when this swellable soft hydrogel is combined with a nonswellable stiff polymer, it endows sufficient strength such that microgrippers structured in this manner are strong enough to excise cells from a tissue clump. On the basis of the stiffness, biocompatibility, biodegradability, and photo-cross-linking of PPF we believe that this is an attractive material for photopatternable soft robotic actuators especially for medical applications. As we have shown, very thin but robust films of

DOI: 10.1021/am508621s
ACS Appl. Mater. Interfaces 2015, 7, 3398−3405

PPF can be created in any desired shape by spin coating and photopatterning.

Our results suggest that since these thermally responsive soft microgrippers actuate around physiological temperatures. The grippers could be stored in a cold solution, allowed to fold completely in one direction, and then deployed with a catheter to a desired location in the body. In the body, this self-folding transition would occur autonomously as the grippers equilibrate from a cold state to physiological temperatures as we achieved previously with metallic microgrippers.

The incorporation of magnetic particles into one or both of the polymeric layers allows the grippers to be remotely directed or retrieved. Since the grippers fold up compactly at both high and low temperatures, they are small enough to be deployed and retrieved using conventional catheters. Further, the compact initial shape would also reduce shear forces in the catheter during deployment. PPF is naturally hydrophobic as is pNIPAM-AAc when the temperature is above 36 °C, suggesting that cells could be grown onto the PPF for other biomedical applications. In cartilage engineering projects, PPF has been incubated in the presence of fetal calf serum to allow the adsorption of proteins onto the surface of PPF to promote cell adherence.[46,47] In addition to cell excision, these magnetic polymeric grippers could be directed and allowed to latch onto specific tissue locations to deliver therapeutics. This can be done by incorporating drugs into either the trigger layer or the stiff segment layer as demonstrated previously.[25]

Finally, we have validated an important design approach for the enabling of relatively stiff stimuli responsive soft-tools by pairing a rigid polymer with a thermoresponsive hydrogel. From a bilayer design perspective, our modeling study shows that there is an optimal thickness ratio and modulus ratio of the active hydrogel layer and the stiff structural layer for the folding angle. Self-folding allows such actuators to respond to stimuli without the need for any wires, tethers, batteries, or power/gas sources. We envision that this approach could also be utilized with other photopatternable or printable biomaterials.[48]

■ ASSOCIATED CONTENT

Supporting Information

Process flow details for fabrication of the PPF/pNIPAM-AAc microgrippers. Details of finite element analysis of gripper folding, parameters for constitutive model, and movies of simulations and grippers folding. This material is available free of charge via the Internet at http://pubs.acs.org

■ AUTHOR INFORMATION

Corresponding Author

*E-mail: dgracias@jhu.edu.

Present Address

[⊥]Center for Bio/Molecular Science and Engineering, U.S. Naval Research Laboratory Code 6900, 4555 Overlook Avenue, SW, Washington, DC, 20375.

Author Contributions

D.H.G. conceived of the study. J.C.B., C.Y., H.R.K. performed experiments. R.X. and T.D.N. performed finite element modeling and analysis. M.O.W. and J.P.F. synthesized the PPF. The manuscript was written through contributions of all authors. All authors have given approval to the final version of the manuscript.

Funding

Funding was provided by the following grants: NSF CBET-1066898, NIH DP2-OD004346−01, NIH R01 AR0614606, NIH R01EB017742, and NIH R01 DE013740.

Notes

The authors declare no competing financial interest.

■ ACKNOWLEDGMENTS

We would like to thank Kate Malachowski for the initial design of the gripper masks, and helpful discussions. We would also like to thank Zhane Rice for help preparing some wafers for polymeric structures. We acknowledge Evin Gultepe's suggestion of incorporation of iron(III) oxide into the polymeric structures to make them ferromagnetic.

■ ABBREVIATIONS

pNIPAM-AAc, poly(*N*-isopropylacrylamide-*co*-acrylic acid)
PPF, polypropylene fumarate
LCST, low critical solution temperature
Si, silicon
DEF, diethyl fumarate
EtOH, ethanol
MeOH, methanol
DI H_2O, deionized water
PVA, poly(vinyl alcohol)
UV, ultraviolet
FEM, finite element model
PBS, phosphate buffered saline
BIS, *N*,*N*-methylenebis-acrylamide
AAc, acrylic acid
φ, weight fraction of dry to swollen gel
$W_{swollen}$, weight of fully swollen sample
W_{dry}, weight of dry sample

■ REFERENCES

(1) Ilievski, F.; Mazzeo, A. D.; Shepherd, R. F.; Chen, X.; Whitesides, G. M. Soft Robotics for Chemists. *Angew. Chem., Int. Ed.* **2011**, *123*, 1930−1935.

(2) Nguyen, N. T.; Ho, S. S.; Low, C. L. N. A Polymeric Microgripper with Integrated Thermal Actuators. *J. Micromech. Microeng.* **2004**, *14*, 969−974.

(3) Chronis, N.; Lee, L. P. Electrothermally Activated SU-8 Microgripper for Single Cell Manipulation in Solution. *J. Microelectromech. Syst.* **2005**, *14*, 857−863.

(4) Carpi, F.; Smela, E. *Biomedical Applications of Electroactive Polymer Actuators*; John Wiley & Sons, Ltd.: New York, 2009; 56−59.

(5) Lu, Y. W.; Kim, C. J. Microhand for Biological Applications. *Appl. Phys. Lett.* **2006**, *89*, 164101.

(6) Mirfakhrai, T.; Madden, J. D. W.; Baughman, R. H. Polymer Artificial Muscles. *Mater. Today* **2007**, *10*, 30−38.

(7) Brown, E.; Rodenberg, N.; Amend, J.; Mozeika, A.; Steltz, E.; Zakin, M. R.; Lipson, H.; Jaeger, H. M. Universal Robotic Gripper Based on the Jamming of Granular Material. *Proc. Natl. Acad. Sci. U.S.A.* **2010**, *107*, 18809−18814.

(8) Stuart, M. A. C.; Huck, W. T. S.; Genzer, J.; Müller, M.; Ober, C.; Stamm, M.; Sukhorukov, G. B.; Szleifer, I.; Tsukruk, V. V.; Urban, M.; Winnik, F.; Zauscher, S.; Luzinov, I.; Minko, S. Emerging Applications of Stimuli-Responsive Polymer Materials. *Nat. Mater.* **2010**, *9*, 101−113.

(9) Randhawa, J. S.; Laflin, K. E.; Seelam, N.; Gracias, D. H. Microchemomechanical Systems. *Adv. Funct. Mater.* **2011**, *21*, 2395−2410.

(10) Gracias, D. H. Stimuli Responsive Self-Folding Using Thin Polymer Films. *Curr. Opin. Chem. Eng.* **2013**, *2*, 112−119.

DOI: 10.1021/am508621s
ACS Appl. Mater. Interfaces 2015, 7, 3398−3405

(11) Ionov, L. Biomimetic Hydrogel-Based Actuating Systems. *Adv. Funct. Mater.* **2013**, *23*, 4555−4570.
(12) Peraza-Hernandez, E. A.; Hartl, D. J.; Malak, R. J.; Lagoudas, D. C. Origami-Inspired Active Structures: a Synthesis and Review. *Smart Mater. Struct.* **2014**, *23*, 094001.
(13) Steinberg, I. Z.; Oplatka, A.; Katchalsky, A. Mechanochemical Engines. *Nature* **1966**, *210*, 568−571.
(14) Maeda, S.; Hara, Y.; Sakai, T.; Yoshida, R.; Hashimoto, S. Self-Walking Gel. *Adv. Mater.* **2007**, *19*, 3480−3484.
(15) Wang, E.; Desai, M. S.; Lee, S.-W. Light-Controlled Graphene-Elastin Composite Hydrogel Actuators. *Nano Lett.* **2013**, *13*, 2826−2830.
(16) Hu, Z. B.; Zhang, X. M.; Li, Y. Synthesis and Application of Modulated Polymer Gels. *Science* **1995**, *269*, 525−527.
(17) Guan, J. J.; He, H. Y.; Hansford, D. J.; Lee, L. J. Self-Folding of Three-Dimensional Hydrogel Microstructures. *J. Phys. Chem. B* **2005**, *109*, 23134−23137.
(18) Shim, T. S.; Kim, S. H.; Heo, C. J.; Jeon, H. C.; Yang, S. M. Controlled Origami Folding of Hydrogel Bilayers with Sustained Reversibility for Robust Microcarriers. *Angew. Chem., Int. Ed.* **2012**, *124*, 1449−1452.
(19) Yuan, B.; Jin, Y.; Sun, Y.; Wang, D.; Sun, J.; Wang, Z.; Zhang, W.; Jiang, X. A Strategy for Depositing Different Types of Cells in Three Dimensions to Mimic Tubular Structures in Tissues. *Adv. Mater.* **2012**, *24*, 890−896.
(20) Thérien-Aubin, H.; Wu, Z. L.; Nie, Z.; Kumacheva, E. Multiple Shape Transformations of Composite Hydrogel Sheets. *J. Am. Chem. Soc.* **2013**, *135*, 4834−4839.
(21) Fusco, S.; Sakar, M. S.; Kennedy, S.; Peters, C.; Bottani, R.; Starsich, F.; Mao, A.; Sotiriou, G. A.; Pané, S.; Pratsinis, S. E.; Mooney, D.; Nelson, B. J. An Integrated Microrobotic Platform for On-Demand, Targeted Therapeutic Interventions. *Adv. Mater.* **2014**, *26*, 952−957.
(22) Bassik, N.; Abebe, B. T.; Laflin, K. E.; Gracias, D. H. Photolithographically Patterned Smart Hydrogel Based Bilayer Actuators. *Polymer* **2010**, *51*, 6093−6098.
(23) Fernandes, R.; Gracias, D. H. Self-Folding Polymeric Containers for Encapsulation and Delivery of Drugs. *Adv. Drug Delivery Rev.* **2012**, *64*, 1579−1589.
(24) Gultepe, E.; Randhawa, J. S.; Kadam, S.; Yamanaka, S.; Selaru, F. M.; Shin, E. J.; Kalloo, A. N.; Gracias, D. H. Biopsy with Thermally-Responsive Untethered Microtools. *Adv. Mater.* **2013**, *25*, 514−519.
(25) Malachowski, K.; Breger, J.; Kwag, H. R.; Wang, M. O.; Fisher, J. P.; Selaru, F. M.; Gracias, D. H. Stimuli-Responsive Theragrippers for Chemomechanical Controlled Release. *Angew. Chem., Int.* **2014**, *126*, 8183−8187.
(26) Yoon, C.; Xiao, R.; Park, J.; Cha, J.; Nguyen, T. D.; Gracias, D. H. Functional Stimuli Responsive Hydrogel Devices by Self-Folding. *Smart Mater. Struct.* **2014**, *23*, 094008.
(27) Schild, H. G. Poly(*N*-isopropylacrylamide): Experiment, Theory, and Application. *Prog. Polym. Sci.* **1992**, *17*, 163−249.
(28) Kim, S.; Healy, K. E. Synthesis and Characterization of Injectable Poly(*N*-isopropylacrylamide-co-acrylic acid) Hydrogels with Proteolytically Degradable Cross- Links. *Biomacromolecules* **2003**, *4*, 1214−1223.
(29) Schmaljohann, D. Thermo-and pH-Responsive Polymers in Drug Delivery. *Adv. Drug Delivery Rev.* **2006**, *58*, 1655−1670.
(30) Peppas, N. A.; Ottenbrite, R. M.; Park, K.; Okano, T. *Biomedical Applications of Hydrogels Handbook*; Springer: New York, 2010.
(31) Siegwart, D. J.; Bencherif, S. A.; Srinivasan, A.; Hollinger, J. O.; Matyjaszewski, K. Synthesis, Characterization, and *In Vitro* Cell Culture Viability of Degradable Poly(N- isopropylacrylamide-co-5,6-benzo-2-methylene-1,3-dioxepane)-based Polymers and Crosslinked Gels. *J. Biomed. Mater. Res., Part A* **2008**, *87A*, 345−358.
(32) Nistor, M.-T.; Chiriac, A. P.; Vasile, C.; Verestiuc, L.; Nita, L. E. Synthesis of Hydrogels Based on Poly(NIPAM) Inserted into Collagen Sponge. *Colloids Surf., B* **2011**, *87*, 382−390.
(33) Guan, Y.; Zhang, Y. PNIPAM Microgels for Biomedical Applications: From Dispersed Particles to 3D Assemblies. *Soft Matter* **2011**, *7*, 6375−6384.
(34) Kasper, F. K.; Tanahashi, K.; Fisher, J. P.; Mikos, A. G. Synthesis of Poly(propylene fumarate). *Nat. Protoc.* **2009**, *4*, 518−525.
(35) Fisher, J. P.; Dean, D.; Mikos, A. G. Photocrosslinking Characteristics and Mechanical Properties of Diethyl Fumarate/Poly(propylene fumarate) Biomaterials. *Biomaterials* **2002**, *23*, 4333−4343.
(36) He, S.; Timmer, M. D.; Yaszemski, M. J.; Yasko, A. W.; Engel, P. S.; Mikos, A. G. Synthesis of Biodegradable Poly(propylene fumarate) Networks with Poly(propylene fumarate)-Diacrylate Macromers As Crosslinking Agents and Characterization of Their Degradation Products. *Polymer* **2001**, *42*, 1251−1260.
(37) Cooke, M. N.; Fisher, J. P.; Dean, D.; Rimnac, C.; Mikos, A. G. Use of Stereolithography to Manufacture Critical-Sized 3D Biodegradable Scaffolds for Bone Ingrowth. *J. Biomed. Mater. Res., Part B* **2002**, *64B*, 65−69.
(38) Martel, S.; Mathieu, J. B.; Felfoul, O.; Chanu, A.; Aboussouan, E.; Tamaz, S.; Pouponneau, P.; Yahia, L.; Beaudoin, G.; Soulez, G.; Mankiewicz, M. Automatic Navigation of an Untethered Device in the Artery of a Living Animal Using a Conventional Clinical Magnetic Resonance Imaging System. *Appl. Phys. Lett.* **2007**, *90*, 114105.
(39) Xi, W.; Solovev, A. A.; Ananth, A. N.; Gracias, D. H.; Sanchez, S.; Schmidt, O. G. Rolled-up Magnetic Microdrillers: Towards Remotely Controlled Minimally Invasive Surgery. *Nanoscale* **2013**, *5*, 1294−1297.
(40) Behkam, B.; Sitti, M. Bacterial Flagella-Based Propulsion and On/Off Motion Control of Microscale Objects. *Appl. Phys. Lett.* **2007**, *90*, 023902.
(41) Kuo, J. C.; Huang, H. W.; Tung, S. W.; Yang, Y. J. A Hydrogel-Based Intravascular Microgripper Manipulated Using Magnetic Fields. *Sens. Actuators, A* **2014**, *211*, 121−130.
(42) Guo, J.; Yang, W. L.; Deng, Y. H.; Wang, C. C.; Fu, S. K. Organic-Dye-Coupled Magnetic Nanoparticles Encaged Inside Thermoresponsive PNIPAM Microcapsules. *Small* **2005**, *1*, 737−743.
(43) Temenoff, J. S.; Mikos, A. G. Injectable Biodegradable Materials for Orthopedic Tissue Engineering. *Biomaterials* **2000**, *21*, 2405−2412.
(44) Lutz, J.-F.; Akdemir, Ö.; Hoth, A. Point by Point Comparison of Two Thermosensitive Polymers Exhibiting a Similar LCST: Is the Age of Poly(NIPAM) over? *J. Am. Chem. Soc.* **2006**, *128*, 13046−13047.
(45) Flory, P. J.; Rehner, J. Statistical Mechanics of Cross-Linked Polymer Networks II. Swelling. *J. Chem. Phys.* **1943**, *11*, 521−526.
(46) Fisher, J. P.; Vehof, J. W. M.; Dean, D.; van der Waerden, J. P. C. M.; Holland, T. A.; Mikos, A. G.; Jansen, J. A. Soft and Hard Tissue Response to Photocrosslinked Poly(propylene fumarate) Scaffolds in a Rabbit Model. *J. Biomed. Mater. Res.* **2002**, *59*, 547−556.
(47) Kim, K.; Dean, D.; Wallace, J.; Breithaupt, R.; Mikos, A. G.; Fisher, J. P. The Influence of Stereolithographic Scaffold Architecture and Composition on Osteogenic Signal Expression with Rat Bone Marrow Stromal Cells. *Biomaterials* **2011**, *32*, 3750−3763.
(48) Lendlein, A.; Langer, R. Biodegradable, Elastic Shape-Memory Polymers for Potential Biomedical Applications. *Science* **2002**, *296*, 1673−1676.

DOI: 10.1021/am508621s
ACS Appl. Mater. Interfaces 2015, 7, 3398−3405